AJNR

Ultra-High-Field MRI Visualization of Cortical Multiple Sclerosis Lesions with T2 and T2*: A Postmortem MRI and Histopathology Study

L.E. Jonkman, R. Klaver, L. Fleysher, M. Inglese and J.J.G. Geurts

AJNR Am J Neuroradiol 2015, 36 (11) 2062-2067
doi: https://doi.org/10.3174/ajnr.A4418
http://www.ajnr.org/content/36/11/2062

Ultra-High-Field MRI Visualization of Cortical Multiple Sclerosis Lesions with T2 and T2*: A Postmortem MRI and Histopathology Study

L.E. Jonkman, R. Klaver, L. Fleysher, M. Inglese, and J.J.G. Geurts

ABSTRACT

BACKGROUND AND PURPOSE: At 7T MR imaging, T2*-weighted gradient echo has been shown to provide high-resolution anatomic images of gray matter lesions. However, few studies have verified T2*WI lesions histopathologically or compared them with more standard techniques at ultra-high-field strength. This study aimed to determine the sensitivity of T2WI and T2*WI sequences for detecting cortical GM lesions in MS.

MATERIALS AND METHODS: At 7T, 2D multiecho spin-echo T2WI and 3D gradient-echo T2*WI were acquired from 27 formalin-fixed coronal hemispheric brain sections of 15 patients and 4 healthy controls. Proteolipid-stained tissue sections (8 μm) were matched to the corresponding MR images, and lesions were manually scored on both MR imaging sequences (blinded to histopathology) and tissue sections (blinded to MR imaging). The sensitivity of MR imaging sequences for GM lesion types and white matter lesions was calculated. An unblinded retrospective scoring was also performed.

RESULTS: If all cortical GM lesions were taken into account, the T2WI sequence detected slightly more lesions than the T2*WI sequence: 28% and 16%, respectively ($P = .054$). This difference disappeared when only intracortical lesions were considered. When histopathologic information (type, location) was revealed to the reader, the sensitivity went up to 84% (T2WI) and 85% (T2*WI) (not significant). Furthermore, the false-positive rate was 8.6% for the T2WI and 10.5% for the T2*WI sequence.

CONCLUSIONS: There is no strong advantage of the T2*WI sequence compared with a conventional T2WI sequence in the detection of cortical lesions at 7T. Retrospectively, a high percentage of lesions could be detected with both sequences. However, many lesions are still missed prospectively. This could possibly be minimized with better a priori observer training.

ABBREVIATIONS: CNR = contrast-to-noise ratio; DIR = double inversion recovery; GML = gray matter lesion; WML = white matter lesion

Multiple sclerosis is traditionally regarded as a chronic inflammatory demyelinating disease of the white matter with a variable clinical course; primary-progressive or relapsing-remitting with possible conversion to secondary-progressive. Pathologic, immunologic, and imaging studies have confirmed that tissue damage in the gray matter is also a key component of the disease process.[1-4] GM pathology occurs frequently, already early in the disease course, and explains cognitive and clinical disability better than white matter lesions.[5,6] Nevertheless, visualizing these GM abnormalities has been challenging due to their small size, absence of inflammation, and partial volume effect from adjacent CSF and WM. The introduction of ultra-high-field MR imaging scanners and specific MR imaging pulse sequences has improved the detection of GM lesions due to a higher signal-to-noise ratio and better spatial resolution.[7-9] 7T T2*-weighted gradient-echo MR imaging has been shown to provide high-resolution anatomic images of GM lesions, and it has even been suggested that this sequence be used as the new criterion standard for GM lesion detection.[10] It was reported to be 44% more sensitive than 1.5T MR imaging in detecting lesions with cortical involvement[11] and up to 69% more sensitive than 3T double inversion recovery (DIR) imaging in detecting subpial lesions.[10]

Few groups have had the opportunity to study GM lesions that were visualized with 7T T2*WI in terms of histopathology. There-

Received February 23, 2015; accepted after revision April 2.

From the Department of Anatomy and Neurosciences (L.E.J., R.K., J.J.G.G.), VU University Medical Center, Amsterdam, the Netherlands; Departments of Radiology (L.F., M.I.), Neurology (M.I.), and Neurosciences (M.I.), Mount Sinai School of Medicine, New York, New York; and Departments of Neuroscience, Rehabilitation, Ophthalmology, Genetics, Maternal and Child Health (M.I.), University of Genoa, Genoa, Italy.

This work was supported by the Dutch MS Research Foundation (grant No. 09-358b) and the US National MS Society (RG 4916A2/1) to M.I. and J.J.G.G. and the Noto Foundation to M.I.

Please address correspondence to L.E. Jonkman, VU University Medical Center, Department of Anatomy and Neurosciences, van der Boechorststraat 7, 1081 BT Amsterdam, the Netherlands; e-mail: le.jonkman@vumc.nl

http://dx.doi.org/10.3174/ajnr.A4418

Table 1: Demographic and neuropathologic data of subjects

Case No.	No[a]	Sex	Age (yr)	PMD (h:min)[b]	DD (yr)	MS Type	COD
MS							
1		M	80	6:05	45	SPMS	Pneumonia
2		F	81	3:30	27	PPMS	Pneumonia
3		M	75	10:10	50	NA	Pneumonia
4		F	66	7:30	17	NA	Pulmonary hypertension
5		M	71	4:00	15	SPMS	Pulmonary carcinoma
6		F	54	6:00	16	SPMS	Liver cancer
7		M	63	4:30	25	SPMS	Pneumonia
8		M	78	3:00	33	SPMS	Euthanasia
9		M	59	5:00	21	SPMS	Euthanasia
10		M	56	10:10	13	NA	Suicide
11		F	56	8:25	32	SPMS	Pneumonia
12		F	54	3:30	31	SPMS	Heart failure
13		M	58	4:00	27	SPMS	Pneumonia
14		F	95	6:30	55	SPMS	Unknown
15		F	81	6:30	21	SPMS	Heart failure
Mean			68.5 ± 12.7	5:56 ± 2:27	28.5 ± 12.9		
Control							
20	4	F	72	>24:00	–	–	Myocardial infarct
21	3	F	58	<24:00	–	–	Breast cancer
22	3	F	76	<24:00	–	–	Pneumonia
23	2	F	76	<8:00	–	–	Pneumonia
Mean			70.5 ± 8.5				

Note:—PMD indicates postmortem delay; DD, disease duration since diagnosis; SPMS, secondary-progressive MS; PPMS, primary-progressive MS; COD, cause of death; NA, unavailable/unknown; –, not applicable.

[a] The numbers indicate number of hemispheric sections included per case.

[b] Control cases are not part of the rapid postmortem examination program and therefore have a longer PMD.

fore, little information is available on the exact sensitivity of T2*WI and/or whether certain lesion types are more visible than others with this sequence. One postmortem study that did look at T2*WI sensitivity showed a 48% prospective sensitivity but made no distinction among lesion types.[12] Another 7T study found that 46% of cortical lesions could be prospectively detected by using T2*WI and a similar 43% could be detected by using a WM-attenuated turbo field echo.[13] However, the 2 sequences studied were suboptimally matched in terms of image resolution, which may explain the relative absence of differences between them. The current study aimed to determine the sensitivity of a standard T2WI and a T2*WI sequence, by using the same image resolution, for detecting MS GM lesion types in postmortem MS tissue.

MATERIALS AND METHODS

Patients and Postmortem Examination

Coronally cut, 10-mm-thick full-hemispheric brain sections of 15 patients with histopathologically confirmed MS (7 women) were selected after rapid postmortem examination (mean postmortem delay, 5 hours 56 minutes) and were formalin-fixed. Additionally, 12 control sections from 4 donors were obtained (recruited and evaluated by the pathology department of VU University Medical Center, Amsterdam, the Netherlands). Table 1 provides demographic and neuropathologic details of the donors. Before death, all donors were registered at the Netherlands Brain Bank, Amsterdam, the Netherlands. All donors gave written informed consent for the use of their tissue and medical records for research purposes. Permission for performing postmortem examinations, use of tissue, and access to medical records was granted by the institutional ethics review board.

MR Imaging

Imaging was performed by using a 7T BioSpec USR70/30 imager (Bruker BioSpin MRI, Ettlingen, Germany), and a vendor-provided 8.6-cm-diameter radiofrequency transmit/receive coil (model 1P T12053V3). Each formalin-fixed brain section was placed into a rectangular plastic tissue container and immersed in 10% buffered formalin. Particular care was devoted to sequence optimization due to the effect of tissue fixation on sequence parameters. The MR imaging protocol included a 2D multiecho spin-echo T2-weighted (TR/TE1/TE2/TE3 = 4000/19.1/38.2/57.3 ms; α = 90 and 180; averages = 6) and a 3D gradient-echo T2*-weighted (TR/TE = 25/12 ms; α = 5; averages = 16) sequence. All MR imaging sequences were acquired with an FOV of 100 × 80, matrix of 1000 × 800, and in-plane spatial resolution of 100 × 100 μm, with a section thickness of 1 mm.

Contrast-to-noise ratios (CNRs) were determined for the different MR image types in the MS samples on the basis of signal-intensity measurements in ROIs (ie, normal-appearing gray matter, GM lesions, normal-appearing white matter, WM lesions, formalin [noise]). The CNR between 2 tissue types was defined as $|SI1 - SI2|/SD$ (*noise*). For T2WI, the TE of 19.1 ms was used for lesion detection and CNR calculation.

Histology

After MR imaging, the brain sections were cut in half to reveal the imaged plane and were embedded in paraffin. Eight-micrometer-thick sections were cut, mounted onto glass slides (Superfrost; VWR International, Leuven, Belgium), and dried overnight at 37°C. Sections were deparaffinized in a series of xylene, 100% alcohol (ethanol), 96% alcohol, and 70% alcohol and rinsed with 0.01-mol/L tris-buffered saline (pH, 7.8–8.0). Endogenous per-

oxidase activity was blocked by incubating the sections in tris-buffered saline with 0.3% H_2O_2 for 30 minutes. After this, the sections were rinsed with 0.01-mol/L phosphate-buffered saline (pH, 7.4). Staining was performed with antibodies against proteolipid protein (AbD Serotec, Oxford, UK) diluted in tris-buffered saline (1:500) containing 1% normal goat serum (Dako, Glostrup, Denmark) and stored overnight at 6°C. Immunolabeling was detected by incubating the sections in biotinylated goat antimouse (1:400; Vector Laboratories, Burlingame, California) and in Vectastain ABC (horseradish peroxidase, 1:200; Vector Laboratories) for 60 minutes at room temperature. Afterward, the sections were washed in 0.05-mol/L tris-hydrochloric acid (pH, 7.6). Peroxidase activity was demonstrated with 0.5-mg/mL 3,3′ diaminobenzidine tetrahydrochloride (DAB; Sigma, St. Louis, Missouri) in 0.01-mol/L tris-hydrochloride containing 0.03% H_2O_2 for 5 minutes, which led to a brown reaction product. Sections were counterstained with hematoxylin (Sigma) and mounted (dePex; BDH Chemicals, Poole, UK).

Scoring, Classification, and Matching

MR imaging lesions were manually marked on all T2*WI, and all T2WI with TE = 19.1 which had contrast similar to that of clinically used T2WI sequences. The MIPAV (National Institutes of Health, Bethesda, Maryland) application was used for manual prospective and retrospective lesion scoring. The MR imaging reader scoring was blinded to clinical information and histopathologic results. Lesions were scored throughout all of the MR imaging slices to avoid bias toward scoring within the sampled areas. A subset of images ($n = 5$ for each sequence) was rated by a second independent reader to ascertain the quality of scoring and calculate an intraclass correlation coefficient for each sequence.

Histopathologically, lesions were defined as areas of complete demyelination (lack of proteolipid protein) and were scored by a histopathologic reader blinded to the clinical and MR imaging data. GM lesions were scored and classified according to criteria described in Bø et al,[14] in which a distinction among 4 cortical lesion types is made. Type I lesions involve the deeper layers of the GM and the adjacent WM; type II lesions are small demyelinated lesions, often centered around blood vessels and confined within the cortex; type III lesions extend from the pial surface into the cortex, most often reaching to cortical layers 3 or 4. When these lesions involve the entire span of the cortex without entering the subcortical white matter, they are defined as type IV lesions. After MR imaging and histopathologic scoring, hemispheric tissue sections were matched to the corresponding MR imaging planes by using WM lesions and as many cortical anatomic landmarks as possible. After the blinded prospective scoring of the postmortem MR imaging and the tissue-to–MR imaging matching, histopathology scores were made available to the MR imaging readers and a second, retrospective, unblinded scoring was performed in consensus between the raters.

Analysis of Data

Histopathologic lesion count was considered the criterion standard. Therefore, prospective and retrospective sensitivity of MR imaging sequences for detecting lesions was determined by dividing the number of lesions scored in the prospective or retrospective ratings by the number of lesions assessed on histopathology, times 100%. The sensitivity of T2WI and T2*WI MR images was statistically compared by using the Wilcoxon signed rank test in SPSS 20.0 (IBM, Armonk, New York). The specificity of MR imaging sequences was determined by dividing the number of false-positives by the number of lesions assessed on histopathology and subtracting this number from 100%. The interrater agreement for prospective lesion detection was expressed as an intraclass correlation coefficient for each sequence (T2WI and T2*WI) by using a 2-way random effects model in absolute agreement. Due to the small number of WM lesions, differences in WM CNRs were kept descriptive. For the difference between GM and gray matter lesion (GML) and between GM and WM (both normally distributed), a paired samples *t* test was performed.

RESULTS

Of the MR imaging–scanned and histopathologically processed samples, 1 section from 1 patient did not show any histopathologic abnormalities and was therefore excluded from analysis. The control sections did not show, apart from age-related frontal capping, any histopathologic abnormalities. The final dataset for analysis included 26 brain sections (from 14 patients and 4 controls). In the MS brain sections, we identified 105 lesions on MR imaging that were verified by histopathology: 7 WM and 98 cortical lesions. Of these cortical lesions, 14 were mixed GM-WM (type I) lesions and 84 were located entirely within the cortical GM (16 type II lesions, 43 type III lesions, and 25 type IV lesions). The intraclass correlation coefficient for the T2WI sequence was 0.972; the intraclass correlation coefficient for the T2*WI sequence was 0.968.

Comparison of Lesion Scoring between T2WI and T2*WI

Results of the histopathologic count and the proportion of lesions detected prospectively and retrospectively on T2WI and T2*WI sequences are shown in Table 2. When focusing on cortical GM lesions (I–IV), the T2WI sequence detected 69% more lesions than T2*WI (Table 2). This difference in GM I–IV lesion detection was not significant ($P = .054$). When only focusing on intracortical GM lesions (II–IV), the T2WI sequence detected 36% more lesions than the T2*WI sequence. This difference was also not significant ($P = .38$). On retrospective scoring, when lesion location was revealed to the MR imaging reader, 81 and 82 cortical lesions were found with the T2WI sequence and T2*WI sequence, respectively, an increase of 200% and 413% compared with prospective scoring. Figure 1 shows matched histologic, T2WI, and T2*WI with prospectively and retrospectively detected lesions. Aside from the detected lesions, we scored 19 false-positives (marked on MR imaging as a lesion but not confirmed by histopathology): 9 on the T2WI sequence and 10 on the T2*WI sequence. This resulted in a specificity of 91.4% for the T2WI and 90.5% for the T2WI sequence. After microscopic inspection of these false-positives, it appeared that many of the cases (89% for T2WI and 80% for the T2*WI sequence) were incompletely demyelinated/remyelinated lesions, which were not scored be-

Table 2: Lesion count and sensitivity of prospective and retrospective MRI scoring[a]

	Histology	Prospective MRI			Retrospective MRI		
Lesion Type	Count	T2WI	T2*WI	*P* Value	T2WI	T2*WI	*P* Value
I	14	8 (57)	2 (14)	–	14 (100)	13 (93)	–
II	16	3 (19)	5 (31)	–	13 (81)	10 (63)	–
III	43	5 (12)	5 (12)	–	32 (74)	36 (84)	–
IV	25	11 (44)	4 (16)	–	22 (88)	23 (92)	–
GML (I–IV)	98	27 (28)	16 (16)	.054	81 (83)	82 (84)	.803
GML (II–IV)	84	19 (23)	14 (17)	.380	67 (80)	69 (82)	0.608
WML	7	6 (86)	3 (43)	–	7 (100)	7 (100)	–
Total	105	33 (31)	19 (18)	.018[b]	88 (84)	89 (85)	.803

Note:— – indicates not statistically assessed.

[a] Sensitivity (in percentages between parentheses) was calculated by dividing the number of lesions scored in the prospective or retrospective ratings by the number of lesions assessed on histopathology, times 100%.

[b] Significant.

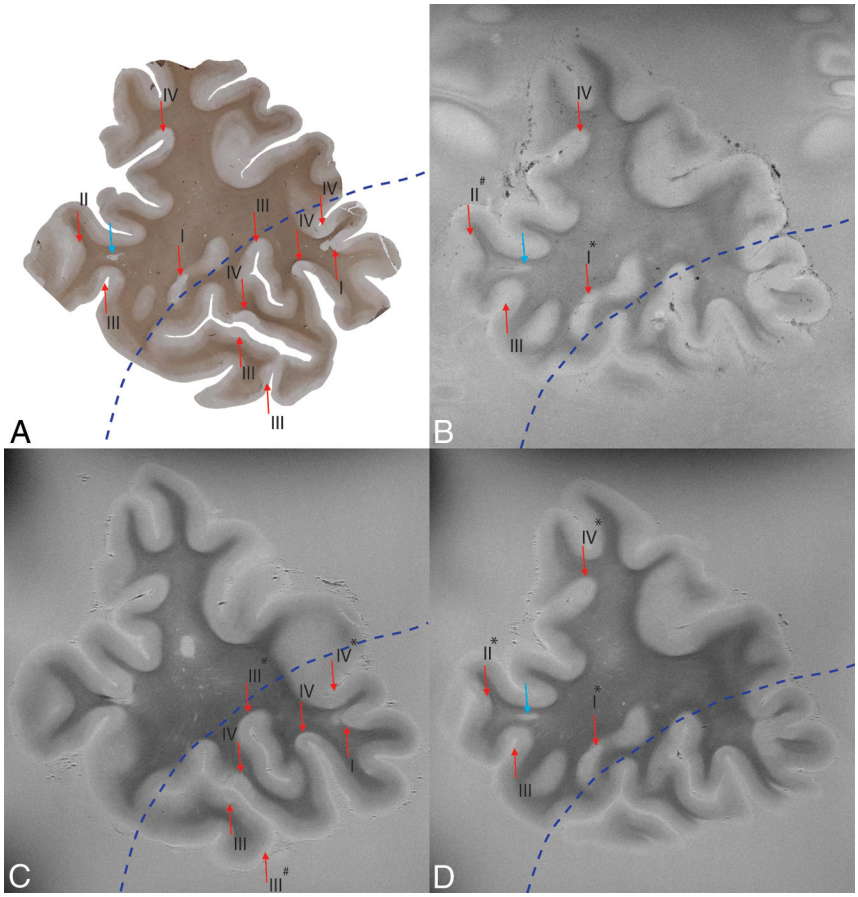

FIG 1. Section stained with anti-proteolipid protein antibodies (*A*), matched with T2*WI (*B*) and T2WI (*C* and *D*). Note that the histologic section corresponds with multiple slices of the MR image; the top part of image *B* and *D* corresponds to the top part of image *A*, and the bottom part of image *C* corresponds to the bottom part of image *A*. The border between successive MR imaging slices is depicted by the *blue dotted line*. Lesions are indicated with *arrows* (WML is blue; GML is red). The type of GM lesion is indicated by I–IV. Also indicated is whether histologic lesions were retrospectively seen on MR imaging (*asterisk*) or missed on MR imaging (*number sign*). All other histologic lesions were prospectively detected. Degree of magnification: 50×.

cause they did not fulfill the criterion of a "fully demyelinated lesion" (see "Materials and Methods").

Contrast-to-noise ratios for the various tissue types are shown in Table 3. Although only descriptive, the T2WI sequence showed higher WM to white matter lesion (WML) CNR, which could account for the higher prospective sensitivity than T2*WI sequence (Table 2). Regarding the T2WI and T2*WI sequences, a paired samples *t* test showed no significant difference between the comparably low GM-GML CNRs.

DISCUSSION

In the current study, we have demonstrated that prospectively (ie, without knowledge of histopathology [location and type of lesions]), the standard T2WI sequence detected more cortical lesions than the T2*WI sequence (ie, 28% versus 16%, respectively), though this difference was not statistically significant. When only intracortical lesions were taken into account, this difference between sequences vanished completely. It also vanished when lesion location was revealed to the reader (retrospective scoring). An explanation for this slight prospective difference could be that the T2*WI sequence is more susceptible to global inhomogeneities such as tissue-to-formalin boundaries, leading to local T2* signal decay,[15] which could hinder prospective lesion detection.

Retrospective detection of cortical lesions increased to 83% for the T2WI and 84% for the T2*WI sequence. When we focused on intracortical lesions, retrospective detection increased to 80% and 82%, respectively. This retrospective detection sensitivity is much higher than that in previous postmortem MR imaging studies at lower field strengths. Previous studies at 1.5T detected only 31%[3] or 56%[16] of intracortical lesions with a T2WI sequence and 29% with a DIR sequence.[17] With a FLAIR sequence, 9%,[17] 21%,[3] or 71%[18] of intracortical lesions were detected retrospectively. Compared with previous postmortem MR imaging studies at ultra-high-field (7T) strength, our T2WI and T2*WI retrospective detection rates are higher than the 67% found with R2* maps,[19] comparable with the 82% found with WM-attenuated turbo field echo, and slightly lower than the 93% detected with T2*WI.[13] However, prospective

Table 3: Contrast-to-noise ratio (±SD)

CNR	T2WI	T2*WI
WM-WML	12.07 (0.90)	5.03 (1.68)
GM-GML	2.01 (0.74)	1.7 (1.37)
GM-WM	7.5 (1.58)	4.96 (3.79)

Note:—WM-WML indicates white matter-to-white matter lesion CNR; GM-GML, gray matter-to-gray matter lesion CNR; GM-WM, gray matter-to-white matter CNR.

lesion detection in these studies varied between 42% and 48%,[13,19] which is higher than our cortical detection rate of up to 28%. One explanation for this higher detection rate in other studies could be the type of lesions identified; most lesions found by Yao et al[19] were the more easily detectable type I lesions, while most lesions in our sample were the more difficult detect type III lesions. Another explanation could be the higher CNR as found in the study by Pitt et al.[13] Their T2*WI sequence had a GML-GM CNR of 3.4, while our study only had an average CNR of 1.7, making distinction between GML and surrounding GM more difficult. These differences could have led to a more optimal sequence for lesion detection by Pitt et al. Future studies should be performed to see how lesion heterogeneity and within-sequence differences influence lesion detection. As shown by the high retrospective lesion count, 7T MR imaging has greatly improved the possibility of detecting cortical or intracortical lesions. However, the challenge remains to actually detect them *prospectively* and *in vivo*.

Regardless of 7T MR imaging with increased signal-to-noise ratio (SNR) and spatial resolution, the number of prospectively detected cortical lesions on MR images remains low; in our study, up to 84% of cortical or intracortical lesions remained undetected. In another study at 7T, up to 57% were still missed.[13] Lesion size has been found to affect the visibility of cortical lesions at both 1.5T[20] and 7T.[13] Furthermore, extensive cortical demyelination could hinder visibility of type IV lesions; when most of the cortex is affected, there is no normal-appearing gray matter present, making it difficult to differentiate areas of demyelination and normal-appearing gray matter (Fig 2). Perhaps quantitative MR imaging could provide additional information in these areas.[21] Automated segmentation could be another option to aid cortical lesion detection, though this could be extremely challenging due to a lack of contrast in the cortex, especially in the upper layers where most cortical lesions are located. Nevertheless, retrospective lesion detection shows that it is possible to find cortical lesions on MR imaging when lesion location is (histopathologically) known, indicating that observer training is important and could dramatically increase future prospective sensitivity.

There were only 7 WMLs observed during histopathologic analysis. This seems low, but the coronal sections were sampled from more frontal regions of the brain, a preferential area for cortical pathology,[22,23] but not far for WMLs, which are more frequently located periventricular.

Sequence parameters were optimized for the effect of fixation, SNR, and spatial resolution. Fixed tissue has a decrease in T2 signal,[24] which leads to lower contrast and requires an increase in averages to achieve a reasonable SNR. This results in an increase in acquisition time, a methodologic limitation when trying to compare the results from this study with the *in vivo* setting. The sequences used can be optimized for the 7T *in vivo* setting, but

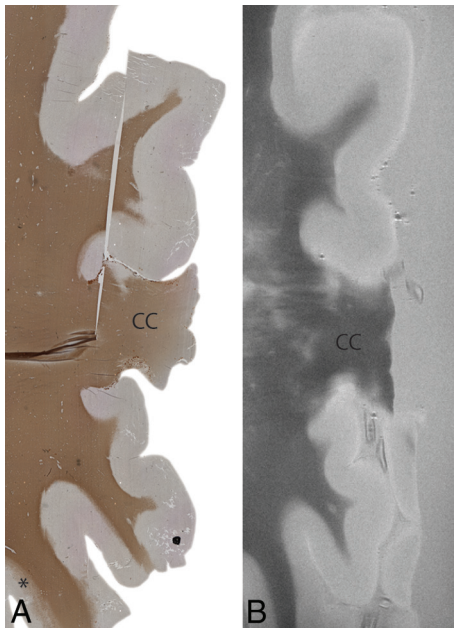

FIG 2. An example of extensive cortical demyelination in an MS case. Histologic section with anti-proteolipid protein antibody (*left*) and a matched T2WI (*right*). The histologic section shows extensive cortical demyelination (lack of proteolipid protein) in the cortex, except for a small section at the left bottom (*asterisk*). This extensive demyelination makes it difficult to differentiate lesions and normal-appearing gray matter on MR imaging (*right*). In this particular case, as a result, prospective MR imaging scoring was negative. CC indicates corpus callosum. Degree of magnification: 50×.

identifying cortical lesions will remain especially challenging for smaller sized lesions.[20] Another limitation in correlative studies between histopathology and MR imaging is matching tissue sections to MR images. Tissue sections were 8 μm, while MR images had a section thickness of 1 mm. However, accurate matching was made possible due to the many anatomic landmarks in the full-hemispheric sections used in this study.

Looking at the in vivo setting, DIR is reported to improve cortical lesion detection at 3T compared with 1.5T, while T2WI or FLAIR is not.[25] In turn, a 75% increase in cortical lesion detection was found with 7T T2WI versus 3T T2WI. For T1 and FLAIR, this was even 91% and 238%, respectively.[26] Another study found a 65% increase in cortical lesion detection with 7T T2*WI versus 3T DIR.[10] The same research group also investigated how various lesion types contributed to physical and cognitive performance. They found that type III–IV lesions had the strongest relationship to physical disability. In turn, type I lesions and, to a lesser extent, type III–IV lesions had a relationship with cognitive performance.[27] At 3T, DIR detected 538% more intracortical lesions than T2WI and 152% more intracortical lesions than FLAIR.[18] This finding was supported by another study in which DIR detected 43% more cortical lesions than FLAIR.[9] However, a study from Kilsdonk et al[28] at ultra-high-field strength (7T) showed that FLAIR detected 89% more cortical lesions than DIR, and that DIR and T2WI obtained nearly identical mean cortical lesion counts (115 versus 116). This finding indicates that a sequence that may be optimal at a lower field strength (DIR at 3T) may lose its benefit at a higher field strength (7T), and vice versa: A sequence suboptimal at a lower field strength may have an advan-

tage over other sequences at higher field strengths (FLAIR or T2* at 7T). It would be useful if future studies could elucidate which sequences have optimal lesion detection sensitivities at which field strength. Phase-sensitive inversion recovery looks promising at 3T with a 307% increase over DIR,[29] but how does it perform at 7T? How do FLAIR, T2WI, and T2*WI compare at 7T in 1 comparative study?

CONCLUSIONS

Our findings suggest that at 7T, T2WI and T2*WI sequences are equally capable of detecting up to 83%–84% of cortical lesions in postmortem MS samples. However, many lesions are still missed prospectively. With observer training, the expectation is that not only the "tip" but a large part of the proverbial "iceberg" of GM lesions may be uncovered.

Disclosures: Laura E. Jonkman—*RELATED*: *Grant*: Dutch MS Research Foundation (09–358b).* Roel Klaver—*RELATED*: Dutch MS Research Foundation.* Matilde Inglese—*RELATED*: *Grant*: National MS Society,* *Comments*: RG 4916A2/1; *UNRELATED*: *Grants/Grants Pending*: Novartis Pharmaceuticals.* Jeroen J.G. Geurts—*RELATED*: *Grant*: Dutch MS Research Foundation. *Money paid to the institution.

REFERENCES

1. Kidd D, Barkhof F, McConnell R, et al. **Cortical lesions in multiple sclerosis.** *Brain* 1999;122(pt 1):17–26 CrossRef Medline
2. Peterson JW, Bö L, Mörk S, et al. **Transected neurites, apoptotic neurons, and reduced inflammation in cortical multiple sclerosis lesions.** *Ann Neurol* 2001;50:389–400 CrossRef Medline
3. Geurts JJ, Blezer EL, Vrenken H, et al. **Does high-field MR imaging improve cortical lesion detection in multiple sclerosis?** *J Neurol* 2008;255:183–91 CrossRef Medline
4. Filippi M, Rocca MA, Calabrese M, et al. **Intracortical lesions: relevance for new MRI diagnostic criteria for multiple sclerosis.** *Neurology* 2010;75:1988–94 CrossRef Medline
5. Roosendaal SD, Moraal B, Pouwels PJ, et al. **Accumulation of cortical lesions in MS: relation with cognitive impairment.** *Mult Scler* 2009;15:708–14 CrossRef Medline
6. Nelson F, Datta S, Garcia N, et al. **Intracortical lesions by 3T magnetic resonance imaging and correlation with cognitive impairment in multiple sclerosis.** *Mult Scler* 2011;17:1122–29 CrossRef Medline
7. Vaughan JT, Garwood M, Collins CM, et al. **7T vs. 4T: RF power, homogeneity, and signal-to-noise comparison in head images.** *Magn Reson Med* 2001;46:24–30 CrossRef Medline
8. Metcalf M, Xu D, Okuda DT, et al. **High-resolution phased-array MRI of the human brain at 7 Tesla: initial experience in multiple sclerosis patients.** *J Neuroimaging* 2010;20:141–47 CrossRef Medline
9. Tallantyre EC, Morgan PS, Dixon JE, et al. **3 Tesla and 7 Tesla MRI of multiple sclerosis cortical lesions.** *J Magn Reson Imaging* 2010;32:971–77 CrossRef Medline
10. Nielsen AS, Kinkel RP, Tinelli E, et al. **Focal cortical lesion detection in multiple sclerosis: 3 Tesla DIR versus 7 Tesla FLASH-T2.** *J Magn Reson Imaging* 2012;35:537–42 CrossRef Medline
11. Kollia K, Maderwald S, Putzki N, et al. **First clinical study on ultra-high-field MR imaging in patients with multiple sclerosis: comparison of 1.5T and 7T.** *AJNR Am J Neuroradiol* 2009;30:699–702 CrossRef Medline
12. Yao B, Bagnato F, Matsuura E, et al. **Chronic multiple sclerosis lesions: characterization with high-field-strength MR imaging.** *Radiology* 2012;262:206–15 CrossRef Medline
13. Pitt D, Boster A, Pei W, et al. **Imaging cortical lesions in multiple sclerosis with ultra-high-field magnetic resonance imaging.** *Arch Neurol* 2010;67:812–18 CrossRef Medline
14. Bø L, Vedeler CA, Nyland HI, et al. **Subpial demyelination in the cerebral cortex of multiple sclerosis patients.** *J Neuropathol Exp Neurol* 2003;62:723–32 Medline
15. Bagnato F, Hametner S, Welch EB. **Visualizing iron in multiple sclerosis.** *Magn Reson Imaging* 2013;31:376–84 CrossRef Medline
16. Geurts JJ, Bö L, Pouwels PJ, et al. **Cortical lesions in multiple sclerosis: combined postmortem MR imaging and histopathology.** *AJNR Am J Neuroradiol* 2005;26:572–77 Medline
17. Seewann A, Kooi EJ, Roosendaal SD, et al. **Postmortem verification of MS cortical lesion detection with 3D DIR.** *Neurology* 2012;78:302–08 CrossRef Medline
18. Geurts JJ, Pouwels PJ, Uitdehaag BM, et al. **Intracortical lesions in multiple sclerosis: improved detection with 3D double inversion-recovery MR imaging.** *Radiology* 2005;236:254–60 CrossRef Medline
19. Yao B, Hametner S, van Gelderen P, et al. **7 Tesla magnetic resonance imaging to detect cortical pathology in multiple sclerosis.** *PLoS One* 2014;9:e108863 CrossRef Medline
20. Seewann A, Vrenken H, Kooi EJ, et al. **Imaging the tip of the iceberg: visualization of cortical lesions in multiple sclerosis.** *Mult Scler* 2011;17:1202–10 CrossRef Medline
21. Samson RS, Cardoso MJ, Muhlert N, et al. **Investigation of outer cortical magnetisation transfer ratio abnormalities in multiple sclerosis clinical subgroups.** *Mult Scler* 2014;20:1322–30 CrossRef Medline
22. Bö L, Geurts JJ, Ravid R, et al. **Magnetic resonance imaging as a tool to examine the neuropathology of multiple sclerosis.** *Neuropathol Appl Neurobiol* 2004;30:106–17 CrossRef Medline
23. Vercellino M, Plano F, Votta B, et al. **Grey matter pathology in multiple sclerosis.** *J Neuropathol Exp Neurol* 2005;64:1101–07 CrossRef Medline
24. Pfefferbaum A, Sullivan EV, Adalsteinsson E, et al. **Postmortem MR imaging of formalin-fixed human brain.** *Neuroimage* 2004;21:1585–95 CrossRef Medline
25. Simon B, Schmidt S, Lukas C, et al. **Improved in vivo detection of cortical lesions in multiple sclerosis using double inversion recovery MR imaging at 3 Tesla.** *Eur Radiol* 2010;20:1675–83 CrossRef Medline
26. de Graaf WL, Kilsdonk ID, Lopez-Soriano A, et al. **Clinical application of multi-contrast 7-T MR imaging in multiple sclerosis: increased lesion detection compared to 3 T confined to grey matter.** *Eur Radiol* 2013;23:528–40 CrossRef Medline
27. Nielsen AS, Kinkel RP, Madigan N, et al. **Contribution of cortical lesion subtypes at 7T MRI to physical and cognitive performance in MS.** *Neurology* 2013;81:641–49 CrossRef Medline
28. Kilsdonk ID, de Graaf WL, Soriano AL, et al. **Multicontrast MR imaging at 7T in multiple sclerosis: highest lesion detection in cortical gray matter with 3D-FLAIR.** *AJNR Am J Neuroradiol* 2013;34:791–96 CrossRef Medline
29. Sethi V, Yousry TA, Muhlert N, et al. **Improved detection of cortical MS lesions with phase-sensitive inversion recovery MRI.** *J Neurol Neurosurg Psychiatry* 2012;83:877–82 CrossRef Medline